SCIAMACHY'S ABSORBING AEROSOL INDEX AND THE CONSEQUENCES OF INSTRUMENT DEGRADATION

L. G. Tilstra[1,2], M. de Graaf[1], S. Noël[3], I. Aben[2], and P. Stammes[1]

[1] *Royal Netherlands Meteorological Institute (KNMI), P.O. Box 201, 3730 AE De Bilt, The Netherlands*
[2] *Netherlands Institute for Space Research (SRON), Sorbonnelaan 2, 3584 CA Utrecht, The Netherlands*
[3] *Institute of Environmental Physics, University of Bremen, FB 1, P.O. Box 330440, D-28334 Bremen, Germany*

Email: l.g.tilstra@sron.nl, graafdem@knmi.nl, stefan.noel@iup.physik.uni-bremen.de, i.aben@sron.nl, stammes@knmi.nl

ABSTRACT

In this paper we present the first results of long-term monitoring the Absorbing Aerosol Index (AAI) [1] measured by the satellite instrument SCIAMACHY [2]. We find a strong increase in the AAI with time, which is found to be caused completely by degradation of the optics. This we conclude from straightforward calculation of the effect of instrument degradation based on available degradation monitoring results. We only studied the scientific product (SC-AAI), not the operational level-2 product (L2-AAI). However, the conclusions we draw in this paper should also apply to the operational level-2 product. We find that the AAI is very sensitive to the absolute calibration of the Earth reflectance, and that a proper absolute calibration, and an accurate correction for the effects of instrument degradation, are essential for this particular product.

Key words: SCIAMACHY; Absorbing Aerosol Index; calibration; degradation.

1. INTRODUCTION

The Absorbing Aerosol Index (AAI) is a dimensionless quantity which was introduced to provide information about the presence of UV-absorbing aerosols in the Earth's atmosphere. It is derived directly from another quantity, the residue, which is defined by [1]

$$r = -100 \cdot \left\{ {}^{10}\log\left(\frac{R_\lambda}{R_{\lambda_0}}\right)^{\rm obs} - {}^{10}\log\left(\frac{R_\lambda}{R_{\lambda_0}}\right)^{\rm Ray} \right\} . \quad (1)$$

In this equation, R_λ denotes the Earth's reflectance at wavelength λ. The superscript $^{\rm obs}$ refers to reflectances which are measured by, in this case, SCIAMACHY, while the superscript $^{\rm Ray}$ refers to modelled reflectances. These modelled reflectances are calculated for a cloud-free and aerosol-free atmosphere where only Rayleigh scattering, absorption by molecules, and Lambertian surface reflection as well as surface absorption can take place.

The reflectance, in this paper, is defined as

$$R = \frac{\pi I}{\mu_0 E} , \quad (2)$$

where I is the radiance reflected by the Earth atmosphere (in $\rm Wm^{-2}nm^{-1}sr^{-1}$), E is the incident solar irradiance at the top of the atmosphere perpendicular to the solar beam (in $\rm Wm^{-2}nm^{-1}$), and μ_0 is the cosine of the solar zenith angle θ_0. As for the wavelengths involved, the wavelengths λ and λ_0 must lie in the UV, and were set to 340 and 380 nm, respectively, for SCIAMACHY.

The Rayleigh atmosphere in the simulations is bounded below by a Lambertian surface having a wavelength independent surface albedo $A_{\rm s}$, which is not meant to represent the actual ground albedo. It is obtained from requiring that the simulated reflectance equals the measured reflectance at λ_0 = 380 nm:

$$R_{\lambda_0}^{\rm obs} = R_{\lambda_0}^{\rm Ray}(A_{\rm s}) . \quad (3)$$

The surface albedo found in this way is used to calculate $R_\lambda^{\rm Ray}$, so one assumes that the surface albedo is constant in the wavelength interval $[\lambda, \lambda_0]$, which is true for most cases. Note that equation 1 can now be reduced to

$$r = -100 \cdot {}^{10}\log\left(\frac{R_\lambda^{\rm obs}}{R_\lambda^{\rm Ray}}\right) . \quad (4)$$

The importance of the residue, as defined above, lies in its ability to effectively detect the presence of absorbing aerosols even in the presence of clouds. When a positive residue ($r > 0$) is found, absorbing aerosols were detected. Negative or zero residues on the other hand ($r \leq 0$), suggest an absence of absorbing aerosols. For that reason, the AAI is defined as equal to the residue r where the residue is positive, and it is not defined where the residue has a negative value.

As an example of the AAI, Fig. 1 presents a global map of the monthly mean SCIAMACHY AAI for June 2004. The results are very similar to the monthly mean found by the TOMS instrument for the same month. The large

Proceedings of the Third Workshop on the Atmospheric Chemistry Validation of Envisat (ACVE-3)
4-7 December 2006, ESRIN, Frascati, Italy (ESA SP-642,February 2007)

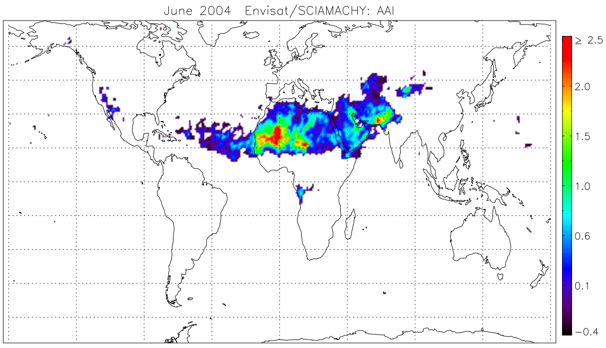

Figure 1. Global map of the monthly mean SCIAMACHY AAI for June 2004. The 'Global Dust Belt' is clearly visible, illustrating the transport of desert dust over the North Atlantic ocean.

plume of UV-absorbing aerosols is called the 'Global Dust Belt'. These are dust aerosols, originating from various desert areas, which are transported westwards over the North Atlantic ocean.

The AAI we present in this paper is not the operational level-2 product (L2-AAI), but the "scientific" product (SC-AAI) based on operational level-1 data, and calculated using our own algorithm. This algorithm uses lookup tables for the simulated reflectance which also include polarisation, identifies sunglint situations, and corrects the reflectance for the known calibration problems of the SCIAMACHY instrument.

2. MONTHLY MEANS OF THE AAI

The SCIAMACHY AAI, and the associated residue, are being monitored on a daily basis and are available on the TEMIS website (http://www.temis.nl). As of the end of 2004, the AAI and the residue are showing abnormally high values [3] (also see Fig. 2). To study this behaviour, we calculated globally averaged and monthly means of the residue for all SCIAMACHY level-1 mission data

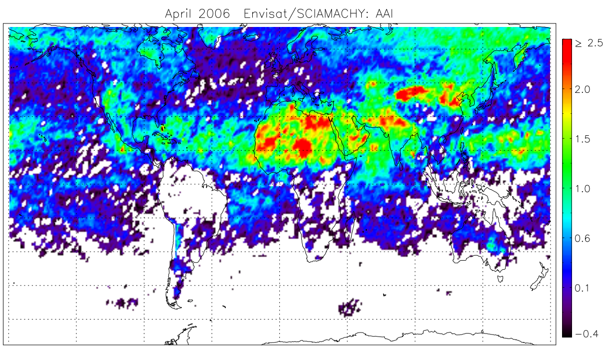

Figure 2. Global map of the monthly mean SCIAMACHY AAI for April 2006. Compared to Fig. 1, the AAI shows anomalously high values. This is caused by degradation of the optics of the SCIAMACHY instrument.

currently available. Note that we do not average the AAI, but the residue. The global monthly mean residue is presented in Fig. 3.

The blue diamonds denote the monthly residue for level-1 data from software versions up to 5.04. These data suffer from a reflectance calibration error in the UV [4], for which was corrected by multiplying the reflectances at 340 and 380 nm by 1.22 and 1.12, respectively. These correction factors had been found from comparing the SCIAMACHY reflectance with that of the radiative transfer code DAK [4]. The blue circles represent level-1 data from software version 6.02. A major calibration change was implemented in going from v5.04 to v6.02 with the aim to remove the aforementioned calibration error. To remove the effects of this calibration change, the reflectances were first scaled back to match the v5.04 calibration. After that, the DAK correction was applied. The black circles, finally, are again the v6.02 data, but now with no corrections applied at all.

Clearly, Fig. 3 confirms that the global monthly residue is increasing with time, where it should be more or less constant. For the GOME instrument [5], a global monthly mean value of -1.2 was found [6]. The data from 2002 and 2003 are therefore found in the proper range, which is indicated by the coloured bar in Fig. 3. This bar also indicates the software versions of the data used. The noisy behaviour of the residue before the start of the year 2005 appears to be related to the fact that the data in this time

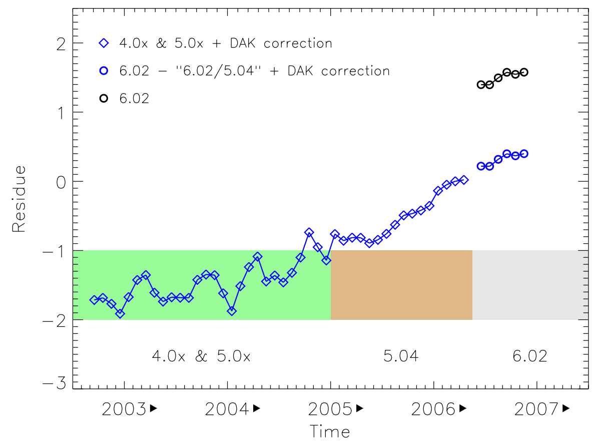

Figure 3. Global Monthly mean SCIAMACHY residue as a function of time. The horizontal bar indicates the software version of the level-1 data. Blue diamonds represent the monthly residue for data handled by data processor versions up to 5.04, calculated after having first performed a correction on the reflectances at 340 and 380 nm. The blue circles relate to version 6.02 data. The reflectances of these data were first scaled back to match the version 5.04 calibration, after which the DAK reflectance correction was applied. The black circles also denote mean residues calculated from version 6.02 data, but now without any correction to the reflectance. Clearly, the global monthly residue is increasing with time, where it should be constant.

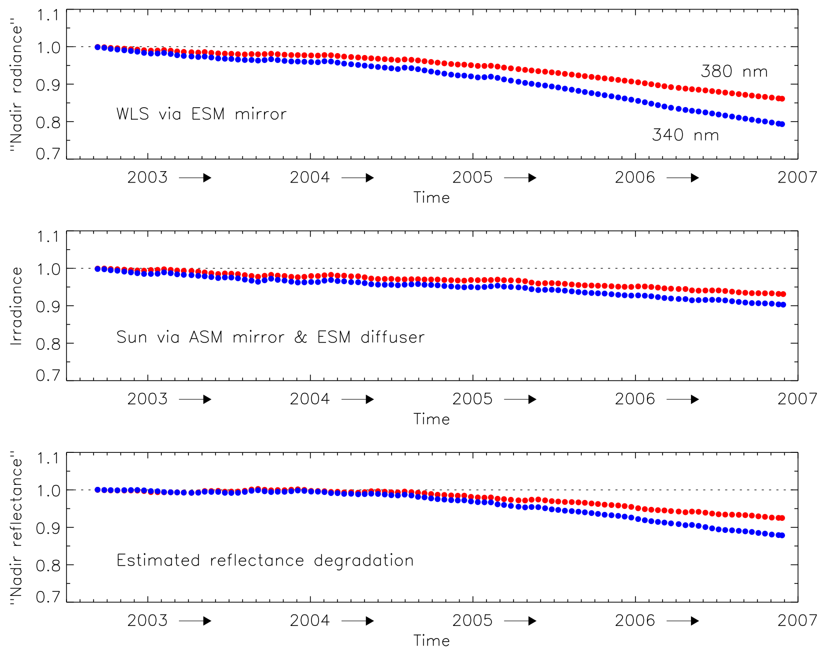

Figure 4. Degradation monitoring result for the two wavelengths relevant to the AAI, i.e. for 340 and 380 nm. The top window presents the signal (normalised to unity at the start of the time series) of the "WLS via ESM mirror" measurements. The light path that is followed for these observations is similar to the light path in normal nadir mode. We therefore consider the signal to record the nadir radiance degradation. The second window shows the irradiance result, and the third window shows the result for the nadir reflectance. Obviously, degradation of the optics has a strong effect for the reflectances at these wavelengths from about the mid of 2004 and onwards.

interval are of various data versions. Starting in 2004, the residue increases rapidly with time, presumably due to degradation of the optics in the SCIAMACHY instrument. We will study the effect of instrument degradation on the residue in the next section.

3. INSTRUMENT DEGRADATION AND AAI

Degradation of the optics in the SCIAMACHY instrument is being monitored regularly, and the results are being made available to the public on the SOST website (http://atmos.caf.dlr.de/projects/scops/). In Fig. 4 we present the recorded degradation for a number of internal instrument light paths, for the wavelengths 340 and 380 nm used for the calculation of the residue. The upper window of the plot shows the recorded signal, as a function of time, that is measured when SCIAMACHY detects its internal lamp (White Light Source, WLS) for degradation monitoring. The signal is normalised to unity for the first available measurement. The light path along the optics in this measurement mode is essentially very similar to the light path followed when the instrument is in normal nadir mode. This suggests that we can consider the curves in the top window of Fig. 4 as representative for the degradation of the nadir radiance.

As expected, the signal of this "nadir radiance" is decreasing with time, due to degradation of the optics. The shorter wavelength (340 nm) is affected more than the longer one (380 nm), which is in line with expectations. The solar irradiance is being measured on a daily basis and the second window of Fig. 4 shows the degradation result (the signal is again normalised to unity). From the "nadir radiance" and the solar irradiance results, we can now construct the "nadir reflectance" (cf. Eq. 2). The result is shown in the bottom window of Fig. 4.

As can be seen, the reflectance has decreased since mid-2004 (by ~10%), depending on the wavelength. This has consequences for the calculation of the residue, via Eqs. 1 and 3. These consequences may be quantified without having to perform a complete recalculation of all the residues, by recognising that changes in the observed reflectances lead to a change in the residue given by

$$\Delta r \approx -100 \cdot {}^{10}\log\left(\frac{c_{340}}{c_{380}}\right) , \qquad (5)$$

where c_{340} and c_{380} are multiplicative factors describing the change in reflectance at the wavelengths in question. Eq. 5 is a first-order approximation, valid only for small values of c_{340} and c_{380}. The degradation factors c_{340} and c_{380} are found directly from the bottom window of Fig. 4.

In Fig. 5 we present a plot similar to Fig. 3. The legend of the latter figure again applies. The added green curve represents Δr, calculated using Eq. 5, and using the factors c_{340} and c_{380} determined from Fig. 4. The red curve represents $r(t_0) + \Delta r$, where $r(t_0)$ is the value of the

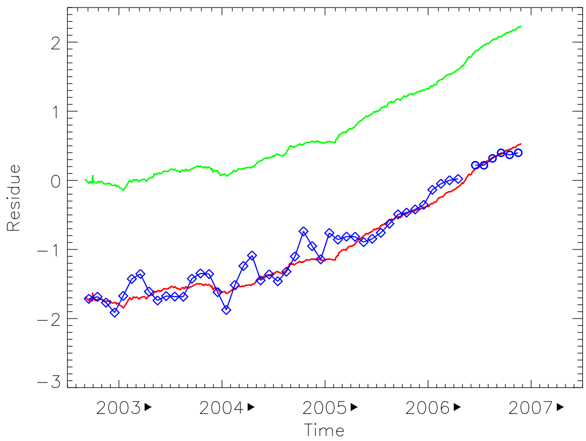

Figure 5. Residue as a function of time. The figure is similar to Fig. 3, and the legend of that figure also applies to this one. The green curve represents Δr, the calculated increase in the residue from degradation of the reflectance alone. The red curve is basically the green curve but then shifted vertically to the value of the global monthly mean residue at the first available data point.

first global monthly mean residue found in Fig. 5 (which is from September 2002). We find that the agreement of the red curve with the time series of the global monthly mean residue is very good.

In other words, the increase in the (global) monthly mean residue can be explained fully by taking degradation of the optics into account. By studying time series of the global monthly mean residue, and by using the light path monitoring results available on the SOST website, we can therefore correct the residue and the AAI very accurately for SCIAMACHY's instrument degradation.

4. CONCLUSIONS

The results show that the increase in the SCIAMACHY AAI, which is derived from the residue, that took place since mid-2004, is completely explained by the effects of degradation of the optics on the nadir reflectance. The results at the same time lend support for the assumption that the degradation of the "WLS via ESM mirror" light path may be interpreted as the degradation of the nadir radiance. A proper absolute calibration of the reflectance and a proper degradation correction are both essential for the quality of the AAI product.

ACKNOWLEDGEMENTS

The work presented in this paper was financed by the Netherlands Agency for Aerospace Programmes (NIVR).

REFERENCES

[1] Herman J.R., Bhartia P.K., Torres O., Hsu C., Seftor C. and Celarier E., Global distributions of UV-absorbing aerosols from Nimbus 7/TOMS data, *J. Geophys. Res.*, Vol. 102, 16,911–16,922, 1997.

[2] Bovensmann H., Burrows J.P., Buchwitz M., Frerick J., Noël S., Rozanov V.V., Chance K.V. and Goede A.P.H., SCIAMACHY: Mission objectives and measurement modes, *J. Atmos. Sci.*, Vol. 56, 127–150, 1999.

[3] de Graaf M. and Stammes P., SCIAMACHY Absorbing Aerosol Index – calibration issues and global results from 2002–2004, *Atmos. Chem. Phys.*, Vol. 5, 2385–2394, 2005.

[4] Tilstra L.G., van Soest G. and Stammes P., Method for in-flight satellite calibration in the ultraviolet using radiative transfer calculations, with application to Scanning Imaging Absorption Spectrometer for Atmospheric Chartography (SCIAMACHY), *J. Geophys. Res.*, Vol. 110, D18311, doi:10.1029/2005JD005853, 2005.

[5] Burrows J.P., et al., The Global Ozone Monitoring Experiment (GOME): Mission concept and first scientific results, *J. Atmos. Sci.*, Vol. 56, 151–175, 1999.

[6] de Graaf M., Stammes P., Torres O. and Koelemeijer R.B.A., Absorbing Aerosol Index: Sensitivity analysis, application to GOME and comparison with TOMS, *J. Geophys. Res.*, Vol. 110, D01201, doi:10.1029/2004JD005178, 2005.